

Testing the presence of QGP in small systems using (multi-)strange hadron correlations with a ϕ meson

Christian Bierlich¹[♣], Stefano Cannito²[◇], Valentina Zaccolo²[♥]

¹ Department of Physics, Lund University, Box 118, SE-221 00 Lund, Sweden

² Department of Physics of the University and INFN Unit, Trieste, Italy

♣ christian.bierlich@fysik.lu.se
◇ stefano.cannito@studenti.units.it
♥ valentina.zaccolo@units.it

Abstract

The study delves into the enhanced production of strange and multi-strange hadrons in proton-proton collisions at LHC. Novel observables are proposed to distinguish between models describing existing data with or without the assumption of a QGP. Two models are explored: EPOS4, based on core-corona separation between a QGP phase and a vacuum phase, and PYTHIA 8.3, based on microscopic interactions between Lund strings. The observables are based on an event selection requiring the presence of a ϕ -meson. Correlations between the ϕ and (multi-)strange hadrons are shown to be an excellent discriminator between the two types of models. These observations emphasize the need for further testing in upcoming LHC Runs, leveraging improved detectors and increased data collection.

1 Introduction

In collisions of heavy nuclei (AA), such as they take place at LHC and RHIC, enhanced production of strange and (multi-)strange hadrons with respect to the e^+e^- baseline, is generally assumed to be a signal of Quark–Gluon Plasma (QGP) production [1–3]. In proton-proton (pp) collisions, the general assumption has historically been that temperature and density is too low for a QGP to form. However, at the LHC it was revealed that small system collisions exhibit several of the same characteristics as collisions of ions [4–8].

When the LHC started up, it was noted by several collaborations [9–11] that the rates of strange mesons and baryons to pions, in minimum bias (MB) collisions, exceeded those expected from LEP [12] and SLD [13], see [14] for a side-by-side comparison. This culminated in the seminal measurements by the ALICE collaboration [8], revealing that not only strangeness is enhanced with respect to the e^+e^- baseline, but also the increase is continuous as function of event multiplicity, and connects smoothly between the smallest multiplicities in pp, with only a single gluon exchange, up to the most central heavy-ion collisions, producing a factor 10^3 more particles at mid-rapidity.

Two very different types of models have performed well in reproducing the rise of strangeness. On the one hand core-corona models [15] where the basic assumption is that droplets of QGP can form down to the smallest collision systems, given that the density is large enough, and on the other hand models of microscopic interactions of strings [16–18] or clusters [19] where fragmentation dynamics is modified by the presence of other strings or clusters. In this paper we will focus on the EPOS4 [20] implementation of the core-corona model [15] and the PYTHIA 8.3 [21] implementation of microscopic interactions, the rope-hadronization model [22].

The current state of affairs, where two types of models with qualitatively different assumptions can explain the same signal, is unsatisfying. The key question to be answered is if there are observables for which a) the two models give very different predictions, that b) can be easily explained in terms of model differences. Crucially, both of these conditions must be met in order for an observable to be a good candidate for measurement. An observable which meets a), but not b), can easily be an artifact from model implementation. Conversely, an observable which meets b) but not a), would place us in the exact same situation as after the original measurement of multi-strange baryons [8].

In this paper, we will develop a series of observables which satisfy both conditions stated above. The observables are based on the observation that while microscopically interacting strings preserve the strangeness quantum number locally (i.e. in each breaking of a string), a macroscopic model will necessarily only preserve it either globally, or locally in some volume of created QGP. Concretely, if a signal is triggered by the presence of a ϕ -meson, a microscopic model will predict a local overabundance of strangeness due to the presence of the ϕ , whereas a QGP based model will not.

The structure of this paper is as follows: in the beginning of Sec. 2 the Lund strings and rope-hadronization model in PYTHIA 8.3, and the core-corona model in EPOS4 will be described. Section 2.3 will explain the role of the ϕ meson trigger in the Lund strings model, and its effects will be explained in Sec. 2.4. Observables to distinguish among the models in strange hadrons production will be shown in Sec. 3, and some final considerations will be drawn in Sec. 4.

2 Two mechanisms for strangeness enhancement

The models for strangeness enhancement in the two generators EPOS4 and PYTHIA 8.3 are very different in nature, with EPOS4 assuming a creation of small volumes of QGP, and PYTHIA 8.3 utilizing the rope formalism. However, they both perform well in reproducing the overall strangeness enhancement results by ALICE [23], as shown in Fig. 1¹. In this section we provide a brief overview of the two models, and point out the main differences, leading up to the development of distinguishing observables in the coming sections.

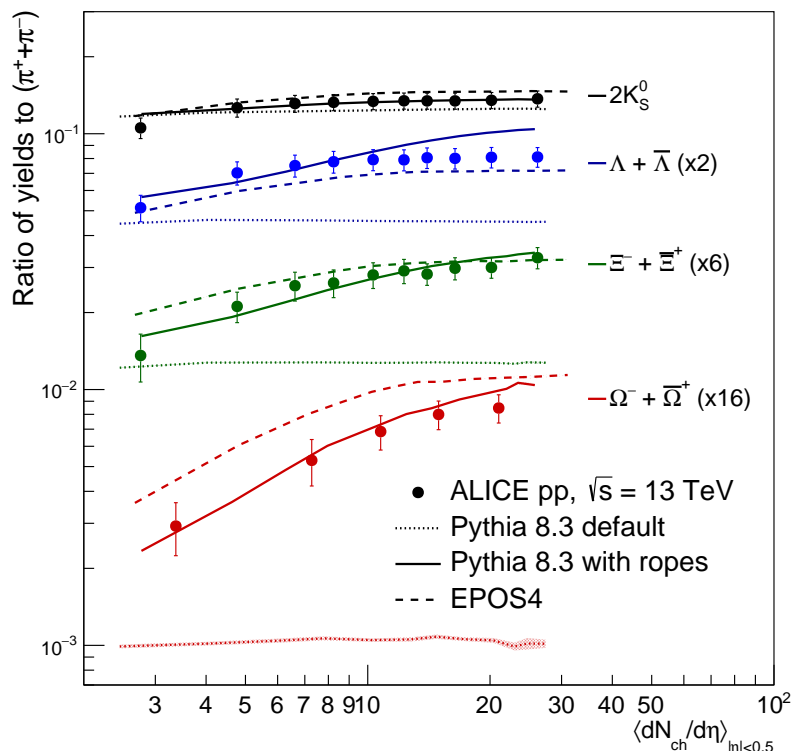


Figure 1: Yield ratios of K_S^0 , $\Lambda + \bar{\Lambda}$, $\Xi^- + \bar{\Xi}^+$ and $\Omega^- + \bar{\Omega}^+$ to $\pi^+ + \pi^-$ in $|y| < 0.5$ as a function of $\langle dN_{ch}/d\eta \rangle_{|y|<0.5}$. Calculations from PYTHIA 8.3 and EPOS4 compared to ALICE results [23] to show that both models do well in describing overall features of strangeness enhancement.

2.1 String and rope hadronization in PYTHIA

The Lund string model is the model underlying hadronization in the PYTHIA 8.3 event generator [21]. Several recent versions include the rope-hadronization model [22] relevant for this study. Both the string model itself and the rope extensions have been thoroughly reviewed in several recent papers (see e.g. [24–26]), and a full review will not be repeated here. However, the most important facets for this study will be outlined in the following.

¹For details pertaining the settings of the two generators see Appendix A.

In PYTHIA 8.3, multiple $2 \rightarrow 2$ parton-parton scatterings radiate off additional quarks and gluons in the parton shower, to finally be hadronized. A $q\bar{q}$ pair will have a string spanned between them, with gluons acting as “kinks” on the string. One string hadronizes to several hadrons, the amount determined by the initial energy of the $q\bar{q}$ pair, and approximately one hadron is produced per unit of rapidity per string.

The hadron flavour is determined by additional $q\bar{q}$ pairs tunneling out of the vacuum when the string breaks (plus the flavour of the two additional end-point quarks). In string breaks, charm quarks are too heavy to be produced in any significant amount, and strange quarks are suppressed with respect to up or down by a factor:

$$\rho = \exp\left(-\frac{\pi(m_s^2 - m_u^2)}{\kappa}\right), \quad (1)$$

where m_s and m_u are the strange and light quark masses respectively, and κ the string tension, which has a numerical value around 1 GeV/fm. In practise, due to uncertainty about which value to use for quark masses, ρ is treated as a free parameter, estimated in e^+e^- collisions at the Z pole, i.e. a single string system. The current default value is $\rho = 0.217$ [21].

When several strings overlap with each other, two things happen, simultaneously. Junction topologies which carry an intrinsic baryon number can be dynamically formed [27, 28], and the effective string tension in the string breaks increases. Starting from the value estimated in e^+e^- , the parameter ρ in eq. 1 will increase as the effective string tension increases [22], giving rise to an enhancement of strange hadrons being formed in high-density environments.

2.2 Core-corona production in EPOS

The core-corona model [15] underlies hadronization in the EPOS4 event generator [20]. In EPOS4, multiple scatterings hadronize, leading to the formation of prehadrons. The density of prehadrons determines the methods that handle the event evolution. If the density of prehadrons is high, as it will commonly be in high multiplicity pp or in AA collisions, they will be treated as core. The core thermalizes and expands collectively. Instead prehadrons close to the surface or escaping the bulk with a large transverse momentum will be treated as corona, i.e. as in vacuum.

The corona part hadronizes using a string model, which is similar to the PYTHIA 8.3 one, but differs in some implementation aspects. One aspect, which is relevant for this project, is that the EPOS4 string does not break as an iterative cascade, where hadrons share break-up quarks. This implies that correlations along the string are different, as it will be elaborated in the following sections.

In the core part, the system is expanded using a hydrodynamic treatment. For this study, the important part of the core evolution is the flavour assignment, which for small systems is performed using a microcanonical approach. In this approach, a volume V with energy E and net flavour content $Q = (n_u - n_{\bar{u}}, n_d - n_{\bar{d}}, n_s - n_{\bar{s}})$, decays into a configuration $\{h_1, \dots, h_n\}$ of hadrons given by the microcanonical partition function [29, 30]:

$$\Omega(\{h_1, \dots, h_n\}) = \frac{V^n}{(2\pi)^{3n}} \prod_{i=1}^n g_i \prod_{\alpha \in S} \frac{1}{n_\alpha!} \int \prod_{i=1}^n d^3 p_i \delta(E - \sum \varepsilon_i) \delta(\sum \vec{p}_i) \delta_{Q, \sum q_i}, \quad (2)$$

where $\varepsilon_i = \sqrt{m_i^2 + p_i^2}$ is the energy, \vec{p}_i the 3-momentum, n_α the number of particles of species α , S the set of particle species considered, g_i the degeneracy of particle i . The δ -function at the end of the partition function is especially relevant for this study. Its role is to ensure flavour conservation, with q_i being the flavour composition of hadron i . The two models are fundamentally different since here the flavour conservation is over the full volume, while in the case of the Lund string, flavour is conserved locally.

2.3 The special role of the ϕ meson

As mentioned in the introduction, the focus in this paper is on discriminating observables making use of the special role of the ϕ meson in the string model, sketched in Fig. 2.

In pp collisions, most strings are aligned with the rapidity axis of the laboratory system. When a ϕ meson is produced, requiring two $s\bar{s}$ string breaks, the leftover (anti-)strange quarks must find their home in hadrons produced in neighboring rank of the same string, i.e. close in rapidity to the ϕ .

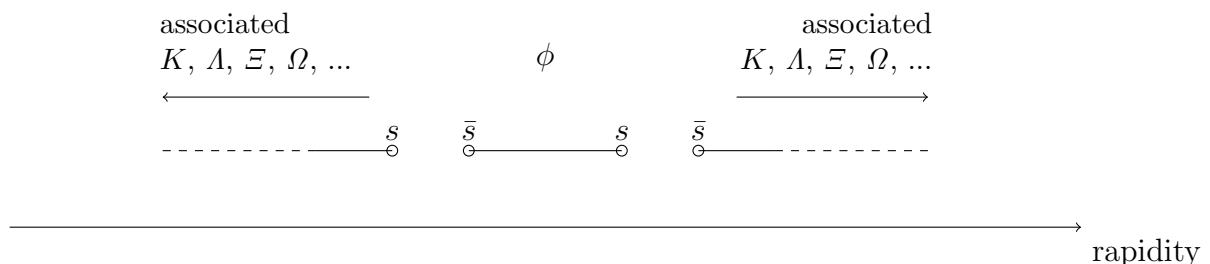


Figure 2: In a pp collision, most strings will be aligned with the rapidity axis of the laboratory frame. When a ϕ meson is produced, it requires two neighboring $s\bar{s}$ string breaks. This, in turn, means that the neighboring (associated) hadrons will include the leftover (anti-)strange quarks from the breakup.

This is a unique prediction of the Lund string model. If the string degrees of freedom would vanish, because they melt into a QGP, the structure carrying the correlations in rapidity would vanish, and the correlations would therefore not be observed.

The explanation given above, holds for a single string. In pp collisions, many strings are produced in the same rapidity interval, and therefore one cannot be certain that a given pair of neighboring particles are produced with string breaks in common, even though they may share quark pairs.

In related methods, such as balance functions [31–33], this is handled by subtraction procedures. Here, however, we are aiming at a method that allows us to highlight directly the qualitative differences arising between the models. A difference will be noticed comparing particle ratios inside the same (high) multiplicity interval, and adding a ϕ trigger to study the same particle ratios inside a narrow rapidity window around the ϕ .

At low multiplicities, on the other hand, where only two strings are present in an event, the addition of a ϕ -trigger has a somewhat more complicated effect.

Take the simplest case of a ϕ produced together with an associated K (either to the left or to the right). Since we have a condition on finding a ϕ in the event, the K/π ratio at low multiplicity will now increase drastically compared to the case with no ϕ trigger. This is simply due to the fact that the additional strange quark has to go somewhere, and the easiest is to end up in a K . Yet again, this is a prediction of the string model, but is not too relevant for distinguishing between QGP production or not, since it is generally not expected at very small multiplicities. It can, however, distinguish between different types of strings, and results about this point will also be shown in Sec. 3 .

2.4 Effects of the ϕ trigger

The main effect of applying a ϕ trigger, will be the emergence of different types of correlations, as outlined in the previous section. Before going to results at final state particle level, we will study whether the application of a ϕ trigger introduces further biases in the model. One could, indeed, imagine that looking in a certain rapidity window around the ϕ would bias the region to have a larger-than-normal string tension, in case of the rope-hadronization model, and a larger fraction of particles produced from the core, in case of core-corona.

For the rope-hadronization model, we study the effective string tension used to produce particles of a given species, with and without applying a ϕ trigger, in the same multiplicity bins as in Fig. 1. In Fig. 3 results are shown for Λ and Ξ (K_S^0 and Ω yield to similar results). In Minimum-bias results (magenta) no ϕ trigger has been applied, in the inclusive sample (black) a ϕ is required to be anywhere in the event, within the selected acceptance ($|y| < 2.5$). The three selections of $|\Delta y|$ signifying that a ϕ meson is required to be within that rapidity range from the particle of interest. These are the same criteria which will be used later for developing final state observables (except for the Minimum-bias curves which correspond to the ones in Fig. 1).

The first thing to notice is that the enhancement in κ_{eff}/κ as a function of multiplicity is different for the two particle species. This is expected since Ξ (with its additional strange valence quark) is easier produced when the string tension is large. Secondly, we notice that the presence of a ϕ is not indicative of a larger local string tension than the one already indicated by the presence of a Λ or a Ξ , except for a very minor effect for Λ at low multiplicity. Finally, the effective string tension rises with multiplicity in both cases, and irrespective of the presence of a ϕ , without saturating at high multiplicities.

In Fig. 4 the same study is repeated for the core-corona model implemented in EPOS4. The quantity of interest in this case is the core fraction, defined as the amount of particles of a given species coming from the core, divided by the total amount of that species in the event. The core fraction is divided in multiplicity bins, as previously for the rope-hadronization model in Fig. 3. The conclusions are similar. The presence of the ϕ does not enhance the core fraction for the particle of interest, although in general the strange baryons are produced more copiously in the core. A noteworthy difference between the two models is that the core fraction saturates at high multiplicities, where the effective string tension does not.

The combined results of Figs. 3 and 4 confirm that the observables presented in the next section will not bias towards a local enhanced string tension or core fraction, but are well suited for studying particle correlations.

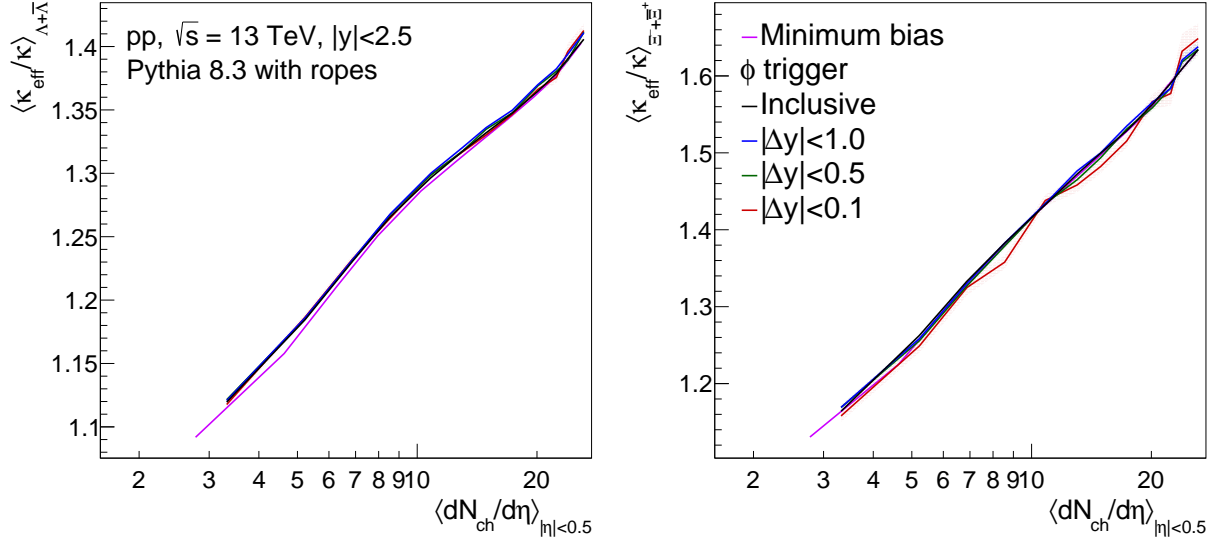


Figure 3: Effective string tension producing $(\Lambda + \bar{\Lambda})$ (left) and $(\Xi^- + \bar{\Xi}^+)$ (right) in $|y| < 2.5$ as a function of $\langle dN_{\text{ch}} / d\eta \rangle$.

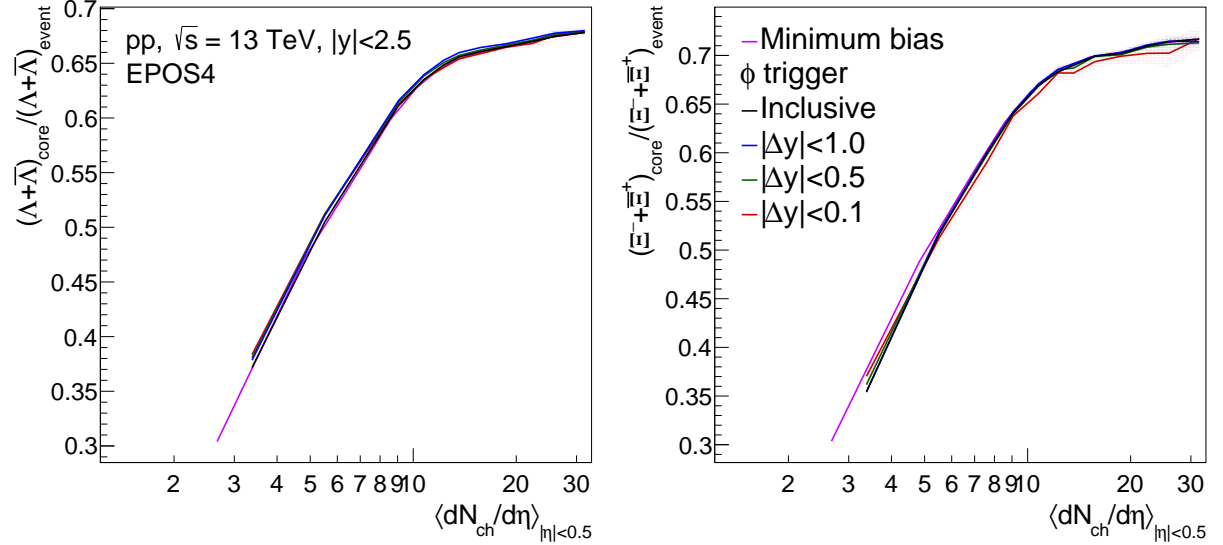


Figure 4: Core fraction of $\Lambda + \bar{\Lambda}$ (left) and $\Xi^- + \bar{\Xi}^+$ (right) in $|y| < 2.5$ as a function of $\langle dN_{\text{ch}} / d\eta \rangle$.

3 Results with final state particles

In this section, the results at hadron level will be discussed. The suggested observables to distinguish between the two types of models are particle ratios in rapidity intervals (Δy) around the triggered ϕ meson.

As in the previous section, the inclusive results (black) indicate that the whole $|y| < 2.5$ is considered, with the presence of a ϕ -meson in the event. All figures shown in this section are thus ratios of (multi-)strange hadron yields to pions, as function of charged-

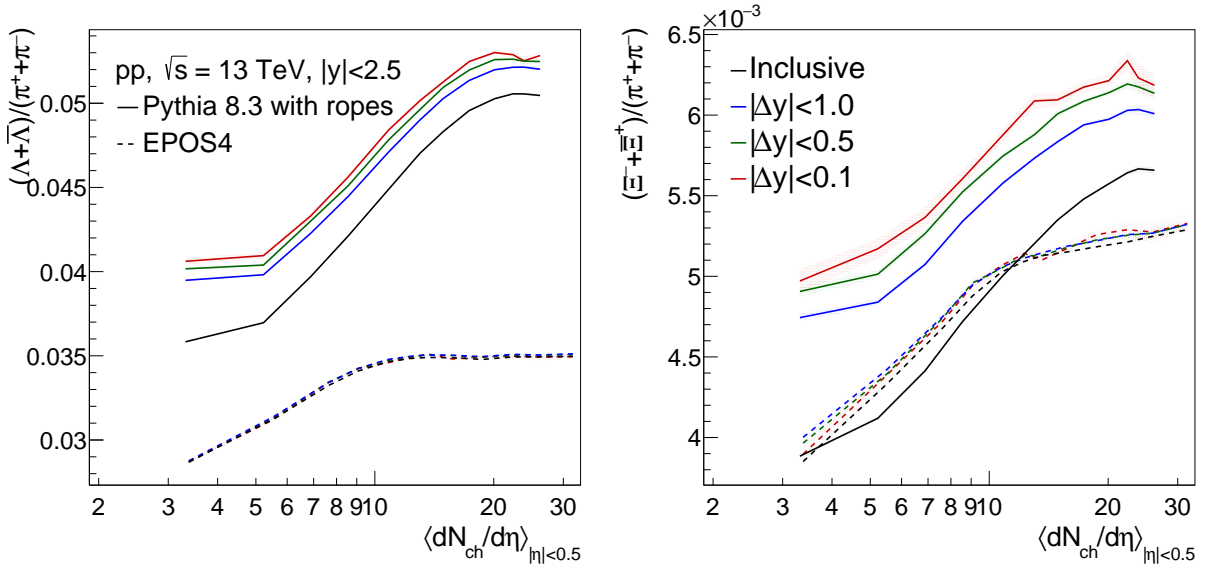


Figure 5: Yield ratios of $(\Lambda + \bar{\Lambda})/(\pi^+ + \pi^-)$ (left) and $(\Xi^- + \bar{\Xi}^+)/(\pi^+ + \pi^-)$ (right) as a function of $\langle dN_{ch}/d\eta \rangle$ in $|\eta| < 0.5$.

particle multiplicity in the rapidity range, $|y| < 2.5$. The coloured lines represent the different rapidity separations between the ϕ meson and the strange hadron of interest, in red $|\Delta y| < 0.1$, in green $|\Delta y| < 0.5$, and in blue $|\Delta y| < 1.0$. PYTHIA 8.3 is shown with fully drawn lines, EPOS4 with dashed lines.

First, in Fig. 5, we show results for Λ (left) and Ξ (right). These hadrons clearly display the features of the models. As the core-corona model is insensitive to local flavour conservation at the level of string breaks, the EPOS4 curves collapse into one single curve. PYTHIA 8.3, on the other hand, observes local flavour conservation at the level of string breaks, and a marked enhancement is clearly seen moving from the inclusive sample, and closer to the ϕ . As one would expect, the effect quickly saturates – the curves for the three $|\Delta y|$ selections are very close together – as hadrons are produced with a separation of one unit of rapidity between them on average².

All curves, for both models, show some degree of saturation at high multiplicities, although this feature is much more noticeable for EPOS4. As shown in the previous section, the core fraction itself saturates (see Fig. 4), giving a natural explanation for EPOS4, where the effective string tension does not (Fig. 3).

In Fig. 6 results for K_S^0 (left) and Ω (right) are shown. These two results are quite different than the ones shown above. The K_S^0 yields with respect to pions are remarkably different. The PYTHIA 8.3 curves rise towards low multiplicities, completely opposite to what one would naively expect from QGP strangeness enhancement and from what one observes in Fig. 1. The explanation lies again in local conservation of strangeness at the level of string breaks. At low multiplicity, there are no baryon junctions. If a ϕ meson is requested the additional strange quark will allow the production of a K (see Fig. 2). In the extreme case of the lowest multiplicity bin with just a few charged particles produced per unit of rapidity, two of those charged particles are likely to be pions from the ϕ decay. This means that it

²The narrow selection in $|\Delta y|$ is motivated by the desire to target a realistic experimental scenario.

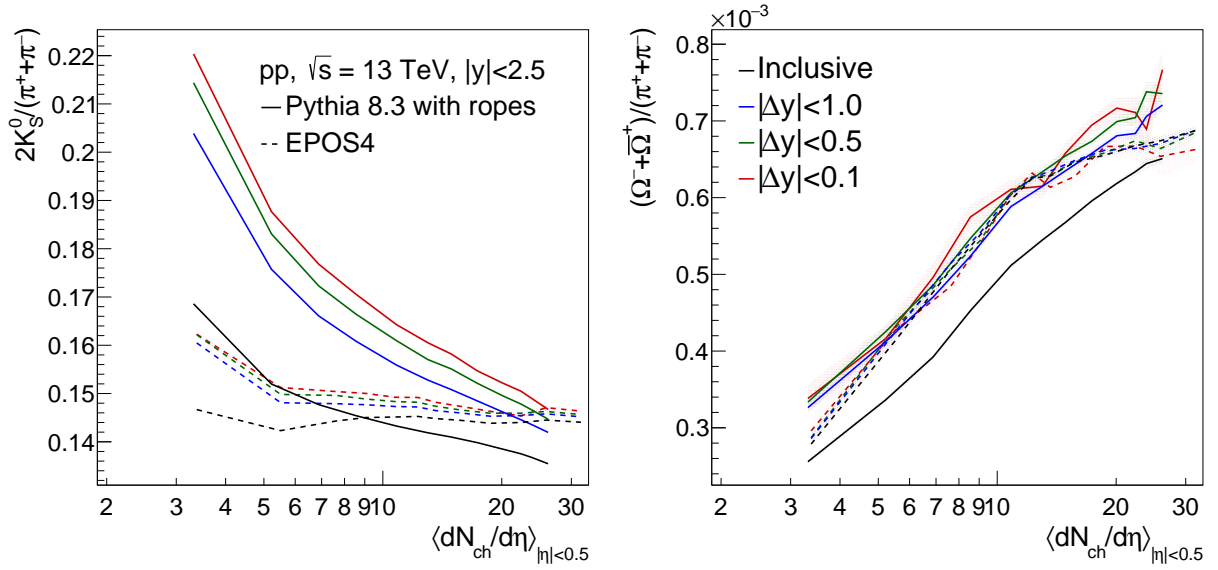


Figure 6: Yield ratios of $2K_S^0/(\pi^+ + \pi^-)$ (left) and $(\Omega^- + \bar{\Omega}^+)/(\pi^+ + \pi^-)$ (right) as a function of $\langle dN_{ch}/d\eta \rangle$ in $|\eta| < 0.5$.

is much more likely to have a K produced on each side of the ϕ , rather than producing a heavily suppressed strange or multi-strange baryon.

The EPOS4 curves are again almost collapsed to a single curve, with a slight bend upwards at low multiplicities. No ingredient in the EPOS4 hadronization model can produce this effect, so it might be attributed to the extreme low multiplicity probed that forces the presence of a handful of charged particles only, a ϕ and a K_0^S in the event.

The result for Ω shown in Fig. 6 (right) is also qualitatively different from the results for Λ and Ξ , shown in Fig. 5. Here all curves are more or less collapsed into a single curve, even though additional strange quarks are, in the case of PYTHIA 8.3, still present from the ϕ production.

The only way to produce the Ω baryon is by production of an ss_1 diquark (subscript indicates spin) followed by an s -quark [34]. The enhancement observed indicates that production of the additional strange quark, once an ss_1 diquark is produced, is not a limiting factor for Ω production. There are no octet baryons with quark content sss , therefore a SU(6) spin \times flavour Clebsch-Gordan weight of zero is assigned to the Ω for the non-existing octet. This means that for Ω in the decuplet the weight will be of unity.

If instead a u or a d quark was produced to combination with the ss_1 diquark, like for the Ξ , the corresponding weights with the same normalization amount to 1/6 in the octet case and 1/3 in the decuplet case. Since these two weights do not sum to unity, but rather to 1/2, it means that one effectively rejects half the u or d string breaks, when they appear next to an ss_1 diquark. Consequently, the regular strangeness suppression factor no longer acts as a suppressor for Ω -production.

Finally, in order to summarize the findings, and thus the suggestions for discriminating observables, we show the four hadron to pion ratios as double ratios in Fig. 7. The double ratios are constructed as the ratio of the original curve to the value integrated over all multiplicity bins. It is clear from this visualization, that curves for all rapidity selections

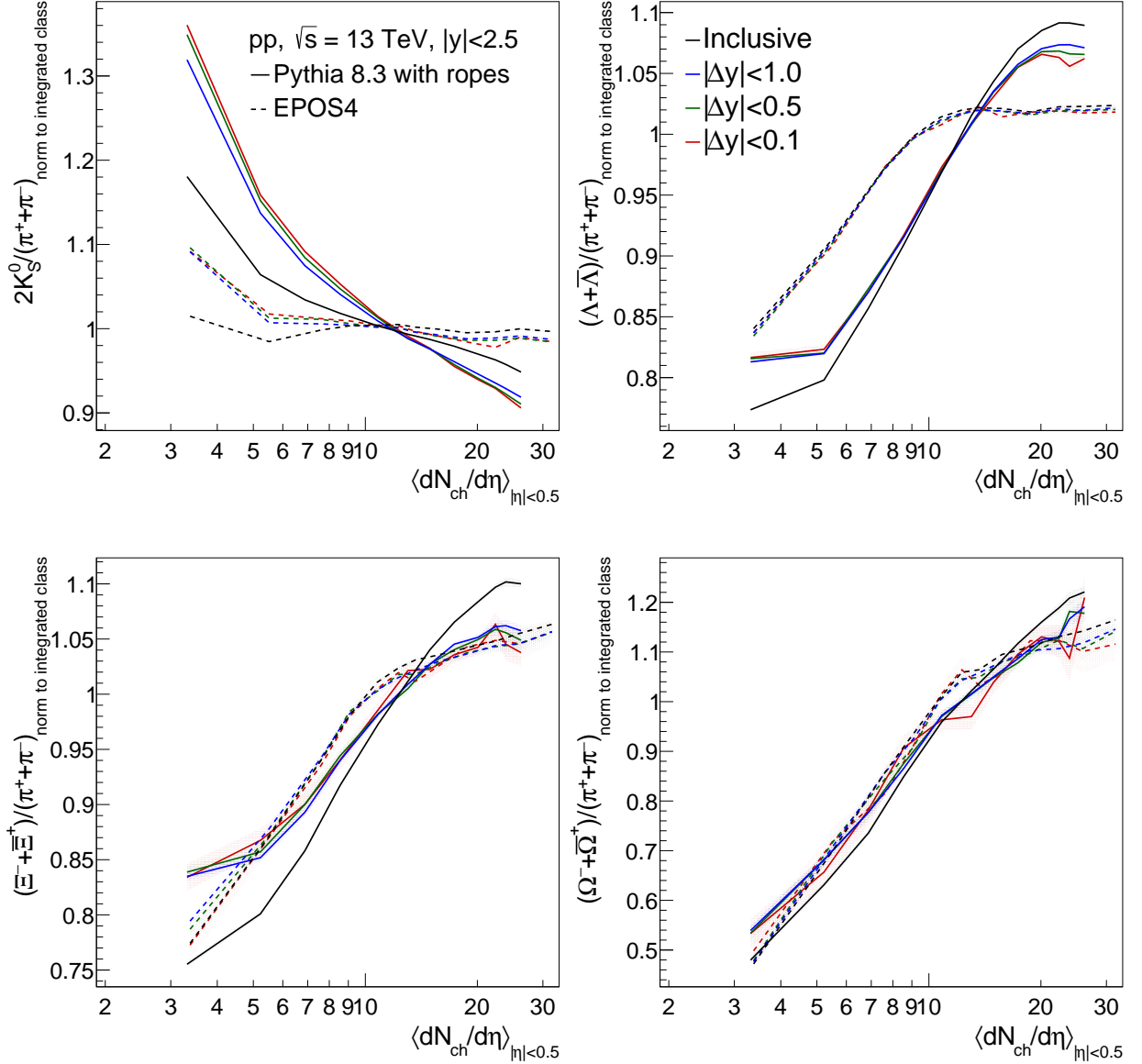


Figure 7: Yield ratios of different strange hadron species measured in $|y| < 2.5$ as a function of $\langle dN_{ch}/d\eta \rangle$ measured in $|\eta| < 0.5$ normalized to the value integrated over all the multiplicity classes: $2K_S^0/(\pi^+ + \pi^-)$ (top left), $(\Lambda + \bar{\Lambda})/(\pi^+ + \pi^-)$ (top right), $(\Xi^- + \bar{\Xi}^+)/(\pi^+ + \pi^-)$ (bottom left) and $(\Omega^- + \bar{\Omega}^+)/(\pi^+ + \pi^-)$ (bottom right).

overlap, indicating that the enhancement is consistent from low to high multiplicity for all the probed rapidity intervals. Beyond that, the double ratios do not reveal many new insights, but serve as a better overview of the potential gain of performing this measurement, with all predictions brought on the same scale.

4 Considerations and outlook

The seminal strangeness enhancement results from ALICE started a whole new direction of research linking flavour enhancement in small and large systems. The apparent ability of microscopic string based models and models based on QGP formation to both describe the data equally well has spurred a large interest in finding observables which can discriminate between the two types of models. In this paper we have developed observables for which the underlying physics differences of the models are highlighted, and that produce significantly different and measurable results.

The different mechanisms for strangeness enhancement implemented in EPOS4 and PYTHIA 8.3 with ropes have been described. It has been shown that studying the strange hadron production in events with a ϕ meson effectively distinguishes among the different strangeness production implementations.

Two main observations are made. Firstly, PYTHIA 8.3 with ropes predicts a clear layering of the strange hadron to pion ratios as a function of the charged particle multiplicity which is not observed in EPOS4. This is expected to originate from the Lund strings and rope-hadronization model. Secondly, the K_0^S/π ratio is decreasing with multiplicity for PYTHIA 8.3 with ropes, remaining rather flat for EPOS4. This is in disagreement with the results both from data and models in the case of MB K_0^S/π ratio, where no ϕ trigger is requested.

Both these observations will have to be tested in data. Run 3 and 4 at LHC open the possibility for such measurements which are statistics eager. Indeed, the amount of data that will be collected will be one to two orders of magnitude larger with respect to the amount of data collected in Run 1 and 2. Another improvement will come from the detector upgrades which will allow to reconstruct particle yields at lower transverse momentum and with higher momentum resolution. Innovative reconstruction algorithms will permit to directly track strange particles, due to vicinity of inner trackers to the beam pipe.

Thanks to all these improvements it will be now possible to detach the different mechanisms that induce strangeness enhancement.

Acknowledgements

Support from the Knut and Alice Wallenberg foundation contract number 2017.0036 (CB and SC), and Vetenskapsrådet contracts 2016-05996 and 2023-04316 (CB) is gratefully acknowledged.

A Event generation parameters

For event generation PYTHIA 8.310³ and EPOS4.0.0 were employed.

The choice parameters for both PYTHIA 8.3 default and with ropes are shown in Tab. 1 and the specific ones for the latter in Tab. 2. EPOS4 parameters are shown in Tab. 3.

PYTHIA 8.3 parameters	
SoftQCD:all	on
ParticleDecays:limitTau0	on
ParticleDecays:tau0Max	10
333:mayDecay	off

Table 1: Parameters used to generate events with both PYTHIA 8.3 default and with ropes.

PYTHIA 8.3 with ropes parameters	
MultiPartonInteractions:pT0Ref	2.15
BeamRemnants:remnantMode	1
BeamRemnants:saturation	5
ColourReconnection:mode	1
ColourReconnection:allowDoubleJunRem	off
ColourReconnection:m0	0.3
ColourReconnection:allowJunctions	on
ColourReconnection:junctionCorrection	1.2
ColourReconnection:timeDilationMode	2
ColourReconnection:timeDilationPar	0.18
Ropewalk:RopeHadronization	on
Ropewalk:doShoving	on
Ropewalk:tInit	1.5
Ropewalk:deltat	0.05
Ropewalk:tShove	0.1
Ropewalk:gAmplitude	0.0
Ropewalk:doFlavour	on
Ropewalk:r0	0.5
Ropewalk:m0	0.2
Ropewalk:beta	0.1
PartonVertex:setVertex	on
PartonVertex:protonRadius	0.7
PartonVertex:emissionWidth	0.1

Table 2: Extra parameters used to generate events with PYTHIA 8.3 with ropes.

³PYTHIA has been subject to minor modifications to allow for extracting the effective string tension.

EPos4 parameters	
MinDecayLength	1.0
nodecays	331
set ninicon	1
core	full
hydro	hlle
eos	x3ff
hacas	off
set nfreeze	100
set centrality	0

Table 3: Parameters used to generate events with EPOS4.

References

- [1] N. Cabibbo and G. Parisi, “Exponential Hadronic Spectrum and Quark Liberation,” *Phys. Lett. B* **59** (1975) 67–69.
- [2] E. V. Shuryak, “Theory of Hadronic Plasma,” *Sov. Phys. JETP* **47** (1978) 212–219.
- [3] **HotQCD** Collaboration, A. Bazavov *et. al.*, “Equation of state in (2+1)-flavor QCD,” *Phys. Rev. D* **90** (2014) 094503, 1407.6387.
- [4] **CMS** Collaboration, V. Khachatryan *et. al.*, “Observation of Long-Range Near-Side Angular Correlations in Proton-Proton Collisions at the LHC,” *JHEP* **09** (2010) 091, 1009.4122.
- [5] **ALICE** Collaboration, B. Abelev *et. al.*, “Long-range angular correlations on the near and away side in p -Pb collisions at $\sqrt{s_{NN}} = 5.02$ TeV,” *Phys. Lett. B* **719** (2013) 29–41, 1212.2001.
- [6] **ATLAS** Collaboration, G. Aad *et. al.*, “Observation of Long-Range Elliptic Azimuthal Anisotropies in $\sqrt{s} = 13$ and 2.76 TeV pp Collisions with the ATLAS Detector,” *Phys. Rev. Lett.* **116** (2016), no. 17 172301, 1509.04776.
- [7] **ATLAS** Collaboration, G. Aad *et. al.*, “Measurement of long-range pseudorapidity correlations and azimuthal harmonics in $\sqrt{s_{NN}} = 5.02$ TeV proton-lead collisions with the ATLAS detector,” *Phys. Rev. C* **90** (2014), no. 4 044906, 1409.1792.
- [8] **ALICE** Collaboration, J. Adam *et. al.*, “Enhanced production of multi-strange hadrons in high-multiplicity proton-proton collisions,” *Nature Phys.* **13** (2017) 535–539, 1606.07424.
- [9] **ALICE** Collaboration, K. Aamodt *et. al.*, “Strange particle production in proton-proton collisions at $\sqrt{s} = 0.9$ TeV with ALICE at the LHC,” *Eur. Phys. J. C* **71** (2011) 1594, 1012.3257.
- [10] **LHCb** Collaboration, R. Aaij *et. al.*, “Prompt K_s^0 production in pp collisions at $\sqrt{s} = 0.9$ TeV,” *Phys. Lett. B* **693** (2010) 69–80, 1008.3105.
- [11] **CMS** Collaboration, V. Khachatryan *et. al.*, “Strange Particle Production in pp Collisions at $\sqrt{s} = 0.9$ and 7 TeV,” *JHEP* **05** (2011) 064, 1102.4282.
- [12] **ALEPH** Collaboration, R. Barate *et. al.*, “Studies of quantum chromodynamics with the ALEPH detector,” *Phys. Rept.* **294** (1998) 1–165.
- [13] **SLD** Collaboration, K. Abe *et. al.*, “Production of π^+ , π^- , K^+ , K^- , p and \bar{p} in Light (uds), c and b Jets from Z^0 Decays,” *Phys. Rev. D* **69** (2004) 072003, hep-ex/0310017.
- [14] C. Bierlich and J. R. Christiansen, “Effects of color reconnection on hadron flavor observables,” *Phys. Rev. D* **92** (2015), no. 9 094010, 1507.02091.

- [15] K. Werner, “Core-corona separation in ultra-relativistic heavy ion collisions,” *Phys. Rev. Lett.* **98** (2007) 152301, 0704.1270.
- [16] T. Sjostrand and B. Soderberg, “A MONTE CARLO PROGRAM FOR QUARK JET GENERATION,”.
- [17] B. Andersson and G. Gustafson, “Semiclassical Models for Gluon Jets and Leptoproduction Based on the Massless Relativistic String,” *Z. Phys. C* **3** (1980) 223.
- [18] B. Andersson, G. Gustafson, and B. Soderberg, “A General Model for Jet Fragmentation,” *Z. Phys. C* **20** (1983) 317.
- [19] B. R. Webber, “A QCD Model for Jet Fragmentation Including Soft Gluon Interference,” *Nucl. Phys. B* **238** (1984) 492–528.
- [20] K. Werner, “Revealing a deep connection between factorization and saturation: New insight into modeling high-energy proton-proton and nucleus-nucleus scattering in the EPOS4 framework,” *Phys. Rev. C* **108** (2023), no. 6 064903, 2301.12517.
- [21] C. Bierlich *et. al.*, “A comprehensive guide to the physics and usage of PYTHIA 8.3,” *SciPost Phys. Codeb.* **2022** (2022) 8, 2203.11601.
- [22] C. Bierlich, G. Gustafson, L. Lönnblad, and A. Tarasov, “Effects of Overlapping Strings in pp Collisions,” *JHEP* **03** (2015) 148, 1412.6259.
- [23] **ALICE** Collaboration, S. Acharya *et. al.*, “Multiplicity dependence of (multi-)strange hadron production in proton-proton collisions at $\sqrt{s} = 13$ TeV,” *Eur. Phys. J. C* **80** (2020), no. 2 167, 1908.01861.
- [24] C. Bierlich, G. Gustafson, and L. Lönnblad, “A shoving model for collectivity in hadronic collisions,” 1612.05132.
- [25] C. Bierlich, G. Gustafson, and L. Lönnblad, “Collectivity without plasma in hadronic collisions,” *Phys. Lett. B* **779** (2018) 58–63, 1710.09725.
- [26] C. Bierlich, “String Interactions as a Source of Collective Behaviour,” *Universe* **10** (2024), no. 1 46, 2401.07585.
- [27] T. Sjostrand and P. Z. Skands, “Baryon number violation and string topologies,” *Nucl. Phys. B* **659** (2003) 243, hep-ph/0212264.
- [28] J. R. Christiansen and P. Z. Skands, “String Formation Beyond Leading Colour,” *JHEP* **08** (2015) 003, 1505.01681.
- [29] K. Werner and J. Aichelin, “Microcanonical treatment of hadronizing the quark - gluon plasma,” *Phys. Rev. C* **52** (1995) 1584–1603, nucl-th/9503021.
- [30] F. M. Liu, K. Werner, and J. Aichelin, “Comparison of microcanonical and canonical hadronization,” *Phys. Rev. C* **68** (2003) 024905, hep-ph/0304174.

- [31] S. A. Bass, P. Danielewicz, and S. Pratt, “Clocking hadronization in relativistic heavy ion collisions with balance functions,” *Phys. Rev. Lett.* **85** (2000) 2689–2692, [nucl-th/0005044](#).
- [32] S. Pratt, “General Charge Balance Functions, A Tool for Studying the Chemical Evolution of the Quark-Gluon Plasma,” *Phys. Rev. C* **85** (2012) 014904, [1109.3647](#).
- [33] **ALICE** Collaboration, S. Acharya *et. al.*, “Studying strangeness and baryon production mechanisms through angular correlations between charged Ξ baryons and identified hadrons in pp collisions at $\sqrt{s} = 13$ TeV,” [2308.16706](#).
- [34] B. Andersson, G. Gustafson, and T. Sjostrand, “A Model for Baryon Production in Quark and Gluon Jets,” *Nucl. Phys. B* **197** (1982) 45–54.